

Article

Interior Melting of the C_3B_{16} and $C_2B_{14}^-$ Clusters Between 1000 K and 2000 K

Li-Ming Yang^{1,2,3,*} and Eric Ganz^{4,*} 

¹ Key Laboratory of Material Chemistry for Energy Conversion and Storage, Ministry of Education, School of Chemistry and Chemical Engineering, Huazhong University of Science and Technology, Wuhan 430074, China

² Hubei Key Laboratory of Bioinorganic Chemistry and Materia Medica, School of Chemistry and Chemical Engineering, Huazhong University of Science and Technology, Wuhan 430074, China

³ Hubei Key Laboratory of Materials Chemistry and Service Failure, School of Chemistry and Chemical Engineering, Huazhong University of Science and Technology, Wuhan 430074, China

⁴ Department of Physics, University of Minnesota, 115 Union St., SE, Minneapolis, MN 55416, USA

* Correspondence: lmyang.uio@gmail.com (L.-M.Y.); ganzx001@umn.edu (E.G.)

Received: 24 October 2017; Accepted: 23 November 2017; Published: 27 November 2017

Abstract: For bulk three-dimensional materials, it is common for the surface to melt at a slightly lower temperature than the bulk. This is known as surface melting, and is typically due to the fact that there are fewer bonds to surface atoms. However, for small clusters, this picture can change. In recent years, there have been investigations of the B_{19} and B_{19}^- clusters, which show striking diffusive behavior as they are heated to 1000 K. We wondered what the effect of substituting a few carbon atoms would be on the properties of these small clusters. To this end, we carried out extensive structural searches and molecular dynamics simulations to study the properties of C_3B_{16} and $C_2B_{14}^-$ at elevated temperatures. The ground state structures and lowest energy isomers for these clusters were determined and calculated. The lowest energy structures are two-dimensional with vacancies inside. The C atoms are located in the outer ring in the ground state. At 1400 K, the outer rim containing the carbon atoms has fixed bonding, while the interior atoms are able to diffuse freely. Therefore, both of these clusters display interior melting at 1400 K. This interior melting is explained by the larger bond strength of the rim atoms. Molecular dynamics simulations at 3000 K showed complete melting and we observed a wide variety of configurations in both clusters.

Keywords: boron clusters; boron-carbon mixed clusters; density functional theory; melting

1. Introduction

For bulk three-dimensional materials, it is common for the surface to melt at a slightly lower temperature than the bulk. This is known as surface melting, and is typically due to the fact that there are fewer bonds to surface atoms [1]. However, for small clusters this picture can change. Recently, there have been investigations of the B_{19} and B_{19}^- clusters which show striking diffusive behavior as they are heated to 1000 K. We wondered what the effect of substituting a few carbon atoms would be on the properties of these small clusters. To this end, we carried out extensive structural searches and molecular dynamics simulations to study the properties of C_3B_{16} and $C_2B_{14}^-$ at elevated temperatures.

Wang and Boldyrev's groups studied B_{19}^- . They found a planar structure, and theoretical calculations showed that the global minimum of B_{19}^- is a nearly circular planar structure with a central B_6 pentagonal unit bonded to an outer B_{13} ring [2]. They also studied B_{16}^{2-} with 10 π -electrons, which is an interesting all-boron analogue of naphthalene [3].

In 2015, Wang et al. found that a B_{11}^- cluster at elevated temperatures can have the outer ring of atoms move freely like a tank tread [4]. In 2017, Wang et al. studied why nanoscale tank treads move

in the doped boron cluster $B_{10}C$ [5]. Jalife et al. also studied the dynamic behavior of planar boron clusters. They observed an interesting rotation of inner rings of atoms compared to outer rings [6]. Zhai and co-workers reported dual dynamic modes in binary clusters [7]. They also studied the Mg_2B_8 cluster, which can be considered a nanoscale compass [8].

Several other studies of dynamics in small B clusters have been reported. Jiménez-Halla et al. published the observation of a B_{19}^- aromatic wankel motor [9]. Internal rotation in B_{13}^+ was studied with chemical bonding analysis [10], and activated with a laser [11]. Further work includes Reference [12]. In 2014, a single C atom substitution into B_{19}^- shut down the fluxionality in the anion [13]. One carbon atom substituted into the structure (in the neutral CB_{18}) enforced bond localization.

Wang and colleagues published a comprehensive review article on planar B clusters in 2016 [14]. They discussed photoelectron spectroscopy of size-selected boron clusters from planar structures to borophenes and borospherenes. They found that interior holes or vacancies are only seen in the ground state when you reach a minimum size of B_{20}^- . Wang et al. observed dynamic fluxionality in a B_{15}^+ cluster, and they labeled this a nanoscale double-axle tank tread [15]. Borospherene (B_{40}) is predicted to act as a support-free spherical two-dimensional liquid at moderate temperatures [16]. In other words, B_{40} could be called a nanobubble.

There has also been a study of a small mixed C and B cluster CB_6 , which found that the C avoids hyper coordination [17]. Wang's group also investigated the doping of B clusters with transition metals. For example, the planar CoB_{18}^- cluster was examined as an example of metallo-borophenes [18]. Liu et al. studied IrB_{12}^- and changed a rigid boron B_{12} platelet to a Wankel motor [19].

There are a large number of techniques for comprehensive geometrical searches for the structures of small clusters. A review of the literature, as well as a recent example of a first principles molecular structural search using genetic algorithms, is described by Supady et al. [20].

In this paper, we examine the result of substituting two or three C atoms into small B clusters. In particular, 20,000 possible configurations were examined in a comprehensive search for the ground state and low-level excited states of $C_2B_{14}^-$ and C_3B_{16} . Due to the large computational cost of the comprehensive searches with these large clusters, two representative clusters of different sizes were chosen for study (one neutral and one ionized). In both cases, the ground state configurations are flat with the C atoms around the edges. Internal vacancies are observed in the ground states. These vacancies permit the inner atoms to move freely at temperatures of 1000 K and 2000 K in density functional theory (DFT) molecular dynamics simulations. At 3000 K, both clusters were fully melted and displayed a wide variety of configurations.

2. Computational Methods

The geometric search was performed using Gaussian, with starting configurations generated at random using the coalescence kick method (CK-Search) [21,22]. This method has been employed successfully by many groups to study small clusters. DFT was used at the PBE1PBE/3-21G and higher levels. Approximately 20,000 geometries were produced for both $C_2B_{14}^-$ and C_3B_{16} . Then ~15,000 geometries were optimized in each case at the 3-21G level. The geometries were then optimized up to the PBE1PBE/6-311+G(d) level. Finally, accurate energies were generated for the 20 lowest structures in each case using Coupled Cluster Single-Double and perturbative triple CCSD(T) theory with 6-311+G(d) basis.

Born–Oppenheimer ab initio molecular dynamics simulations were performed using periodic cells with a single cluster in the center. The unit cell was fixed at $15.0 \text{ \AA} \times 15.0 \text{ \AA} \times 15.0 \text{ \AA}$. The spacing between adjacent cells ensures good isolation. The DFT-D and Tkatchenko–Scheffler (TS) methods were used in CASTEP [23] in Materials Studio 8. A cutoff energy of 280 eV, “fine” parameters, SCF tolerance = 3×10^{-6} , smearing = 0.03, and the Nosé–Hoover thermostat were used.

3. Results and Discussion

In Figure 1, we show the results of the comprehensive geometry search for $C_2B_{14}^-$. The energies are listed at the CCSD(T) level, relative to the ground state at the top left. The ground state for this cluster has 11 B atoms in a compact and flat configuration with the two C atoms located around the outer edge. The system has one C atom with just two double bonds to neighboring B atoms (as determined by bond length in Materials Studio). Unusually, a vacancy is observed in the ground state of the cluster. A similar configuration is also observed with relative energy +1 eV. Surprisingly, the fully compact configuration has an energy of +6.8 eV, and is slightly curved. In all eight of the lowest energy configurations, the two C atoms are located on the outside of the cluster. Hirshfeld charge analysis reveals that most of the charge is located on the C atoms, with a net charge of 0.20e and 0.34e on the two C atoms, respectively.

In Figure 2, the lowest energy configurations for the C_3B_{16} cluster are shown. The ground state is at top left with relative energy 0 eV. The three lowest energy configurations are flat. The next two configurations with relative energy 0.54 eV are curved. The bottom right two configurations at higher energies show a three-dimensional (3D) structure. The carbon atoms are generally located in the outer rim, although the second configuration has one C atom in the center. Vacancies are observed in all of these configurations.

A snapshot from the $C_2B_{14}^-$ molecular dynamics movie at 1400 K is displayed in Figure 3. The bonding configuration stays generally the same during this movie. The outer rim atoms still stay bonded in the same order. Therefore, this cluster shows interior melting at 1400 K. In the supplemental information, movies at 1000 K, 1400 K, 2000 K, and 3000 K for this cluster are available. As the temperature is raised from 1000 K to 2000 K, the exterior atoms stay locked in place, while the interior is liquid. As the temperature is raised, the motion increases, and the clusters fold more. Figure 4 shows the last frame from the 2000 K simulation.

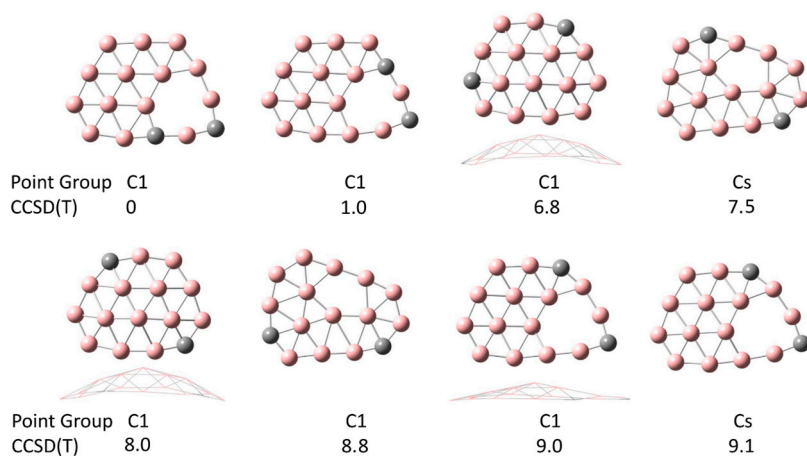


Figure 1. Lowest energy configurations for $C_2B_{14}^-$. Energies in eV are shown relative to the ground state at the top left. These configurations are all relatively flat, with the ground state flat. The carbon atoms are located in the outer rim. Vacancies are observed in most of these configurations.

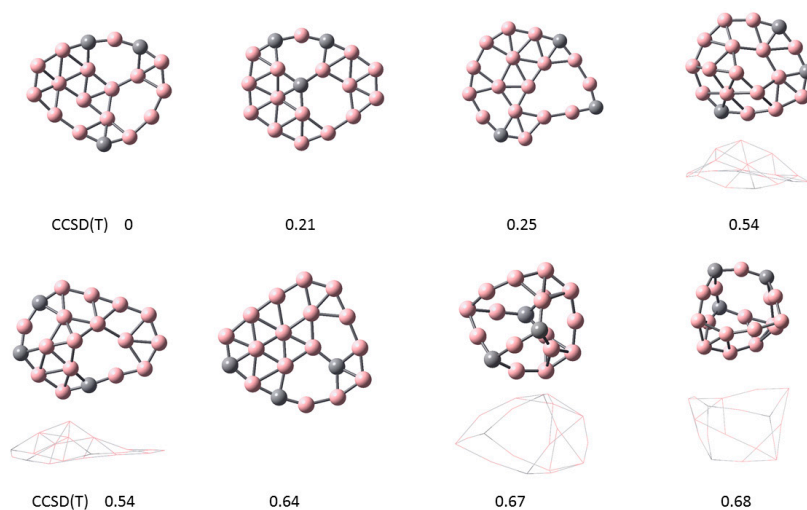


Figure 2. Lowest energy configurations for C_3B_{16} . The ground state is shown at top left with relative energy 0. The three lowest energy configurations are flat. The next two configurations with relative energy 0.54 eV are curved. The bottom right two configurations at higher energies show a three-dimensional (3D) structure. The carbon atoms are generally located in the outer rim, although the second configuration has one C atom in the center.

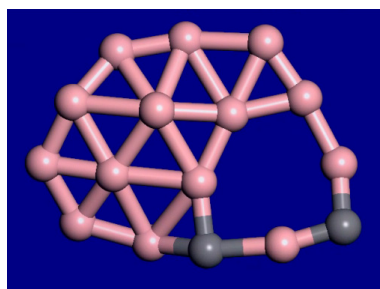


Figure 3. Snapshot from a 10-ps $C_2B_{14}^-$ molecular dynamics movie at 1400 K. The bonding configuration stays generally the same during this movie. The outer rim atoms still stay bonded in the same order.

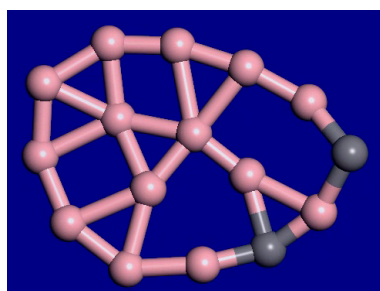


Figure 4. Last frame of the $C_2B_{14}^-$ simulation, 9 ps, 2000 K.

For C_3B_{16} , the molecular dynamics simulations at 1000 K, 1400 K, and 2000 K show that the outer atoms still maintain their relative order, while the inner atoms and vacancies are diffusing around. Therefore, the interior is liquid, while the outer rim is still solid in this temperature range. This cluster has an unusual form of interior melting as opposed to surface melting. Frames at 39 ps and 40 ps from the 1400 K molecular dynamics (MD) simulation are shown in Figure 5. A snapshot from the 40-ps MD movie at 2000 K is shown in Figure 6. The outer rim atoms stay in order. Therefore, this cluster

shows interior melting at 1400 K. Portions of the MD movies at 1000 K, 1400 K, 2000 K, and 3000 K are included in the supplemental material.

The interior melting of these clusters is explained by the unusually large bond strength of the rim atoms. This may be due to several effects, including the two-dimensional (2D) nature of some of the clusters, the presence of C atoms in the rim, and the specific bonding. Stronger bonding of the rim atoms has been observed previously in small 2D B clusters. For boron-based 2D clusters, the rim has relatively strong 2c–2e sigma bonds and delocalized pi and sigma bonds with respect to the interior delocalized pi and sigma bonds [24]. The presence of C atoms primarily in the rim, and the lack of hyper-coordination for C are consistent with and explained by the recent results of Feng and Zhai [25].

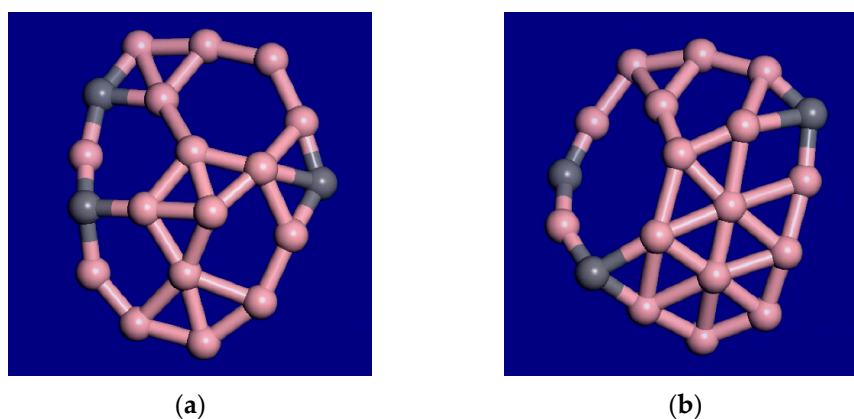


Figure 5. Two snapshots from the C_3B_{16} molecular dynamics movie at 1400 K. (a) is the result at 39 ps, and (b) at 40 ps. The outer rim atoms are able to oscillate, but the outer atoms stay bonded in the same order. The bonding and the inner atoms change as the open areas or vacancies and the atoms diffuse around the interior of the cluster.

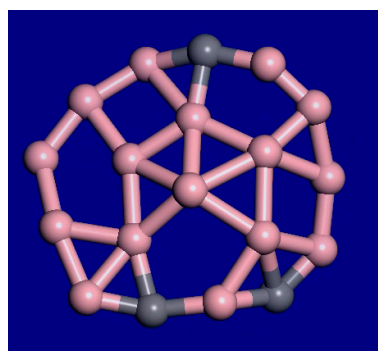


Figure 6. Snapshot from the 40-ps C_3B_{16} molecular dynamics movie at 2000 K. Much more motion is observed, including larger holes and faster changes. The outer rim atoms still stay bonded in the same order.

Molecular dynamics simulations were also carried out at 3000 K to explore the higher temperature regime. At 3000 K, the C_3B_{16} cluster is completely melted. A wide variety of structures are observed including flat two-dimensional structures, compact three-dimensional structures, and mixed or other structures. At some points, carbon atoms are able to penetrate the interior of the cluster. Even after 40 ps, flat 2D structures (with all three carbons on the outside) similar to the ground state structures are still observed. This confirms the results of the comprehensive geometric search. Furthermore, when the system is in one of these flat 2D structures, it is more stable than when it is in one of the other three-dimensional structures. Movies of these high-temperature liquid clusters are included in the

supplemental information. The molecular dynamics simulation of $C_2B_{14}^-$ at 3000 K also shows that the cluster is completely melted and able to access a wide variety of configurations.

4. Conclusions

In this paper, we examined the result of substituting two or three C atoms into small B_{16} and B_{19} clusters. Using extensive computation, 20,000 possible configurations were examined in a comprehensive search for the ground state and low-level excited states of $C_2B_{14}^-$ and C_3B_{16} . The ground state configurations are flat with the C atoms around the edges. Low symmetry structures and unusual two-dimensional structures were found. The energies of the lowest excited states were accurately determined. Unusual vacancies were observed in the ground states. These vacancies permit the inner atoms to move freely at temperatures between 1000 K and 2000 K in DFT molecular dynamics simulations. Therefore, both clusters display unusual interior melting in this temperature range. This interior melting is due to the increased bonding strength of the outer rim atoms. At 3000 K, both clusters were completely melted, and were able to access a wide variety of configurations. Molecular dynamics movies are available in the supplemental information.

Supplementary Materials: Molecular dynamics movies of the simulations are available available online at <http://www.mdpi.com/2410-3896/2/4/35/s1>. Note that the two clusters have different frame rates in the movies.

Acknowledgments: We thank the Minnesota Supercomputer Institute for computational support. Li-Ming Yang gratefully acknowledges the support from startup fund (2006013118 and 3004013105) and independent innovation research fund (0118013090) from the Huazhong University of Science and Technology, and the National Natural Science Foundation of China (Grant no. 21673087).

Author Contributions: Li-Ming Yang carried out the configuration search, while Eric Ganz carried out the molecular dynamics. Both authors collaborated on all elements of the paper, including planning the research.

Conflicts of Interest: The authors declare no conflict of interest.

References

1. Frenken, J.W.; van der Veen, J.F. Observation of Surface Melting. *Phys. Rev. Lett.* **1985**, *54*, 134–137. [[CrossRef](#)] [[PubMed](#)]
2. Huang, W.; Sergeeva, A.P.; Zhai, H.-J.; Averkiev, B.B.; Wang, L.-S.; Boldyrev, A.I. A Concentric Planar Doubly π -Aromatic B_{19}^- Cluster. *Nat. Chem.* **2010**, *2*, 202–206. [[CrossRef](#)] [[PubMed](#)]
3. Sergeeva, A.P.; Zubarev, D.Y.; Zhai, H.-J.; Boldyrev, A.I.; Wang, L.-S. A Photoelectron Spectroscopic and Theoretical Study of B_{16}^- and B_{16}^{2-} : An All-Boron Naphthalene. *J. Am. Chem. Soc.* **2008**, *130*, 7244–7246. [[CrossRef](#)] [[PubMed](#)]
4. Wang, Y.-J.; Zhao, X.-Y.; Chen, Q.; Zhai, H.-J.; Li, S.-D. $B_{11}(-)$: A Moving Subnanoscale Tank Tread. *Nanoscale* **2015**, *7*, 16054–16060. [[CrossRef](#)] [[PubMed](#)]
5. Wang, Y.-J.; Guo, J.-C.; Zhai, H.-J. Why Nanoscale Tank Treads Move? Structures, Chemical Bonding, and Molecular Dynamics of a Doped Boron Cluster $B_{10}C$. *Nanoscale* **2017**, *9*, 9310–9316. [[CrossRef](#)] [[PubMed](#)]
6. Jalife, S.; Liu, L.; Pan, S.; Cabellos, J.L.; Osorio, E.; Lu, C.; Heine, T.; Donald, K.J.; Merino, G. Dynamical Behavior of Boron Clusters. *Nanoscale* **2016**, *8*, 17639–17644. [[CrossRef](#)] [[PubMed](#)]
7. Guo, J.-C.; Feng, L.-Y.; Wang, Y.-J.; Jalife, S.; Vásquez-Espinal, A.; Cabellos, J.L.; Pan, S.; Merino, G.; Zhai, H.-J. Coaxial Triple-Layered versus Helical $Be_6B_{11}^-$ Clusters: Dual Structural Fluxionality and Multifold Aromaticity. *Angew. Chem.* **2017**, *129*, 10308–10311. [[CrossRef](#)]
8. Wang, Y.-J.; Feng, L.-Y.; Guo, J.-C.; Zhai, H.-J. Dynamic Mg_2B_8 Cluster: A Nanoscale Compass. *Chem. Asian J.* **2017**, *12*, 2899–2903. [[CrossRef](#)] [[PubMed](#)]
9. Jiménez-Halla, J.O.C.; Islas, R.; Heine, T.; Merino, G. B_{19}^- : An Aromatic Wankel Motor. *Angew. Chem. Int. Ed.* **2010**, *49*, 5668–5671. [[CrossRef](#)] [[PubMed](#)]
10. Martínez-Guajardo, G.; Sergeeva, A.P.; Boldyrev, A.I.; Heine, T.; Ugalde, J.M.; Merino, G. Unravelling Phenomenon of Internal Rotation in B_{13}^+ through Chemical Bonding Analysis. *Chem. Commun.* **2011**, *47*, 6242–6244. [[CrossRef](#)] [[PubMed](#)]
11. Merino, G.; Heine, T. And Yet It Rotates: The Starter for a Molecular Wankel Motor. *Angew. Chem. Int. Ed.* **2012**, *51*, 10226–10227. [[CrossRef](#)] [[PubMed](#)]

12. Moreno, D.; Pan, S.; Zeonjuk, L.L.; Islas, R.; Osorio, E.; Martínez-Guajardo, G.; Chattaraj, P.K.; Heine, T.; Merino, G.; Su, S.J.; et al. B_{18}^{2-} : A Quasi-Planar Bowl Member of the Wankel Motor Family. *Chem. Commun.* **2014**, *50*, 8140–8143. [[CrossRef](#)] [[PubMed](#)]
13. Cervantes-Navarro, F.; Martínez-Guajardo, G.; Osorio, E.; Moreno, D.; Tiznado, W.; Islas, R.; Donald, K.J.; Merino, G.; Merino, G. Stop Rotating! One Substitution Halts the B_{19}^- Motor. *Chem. Commun.* **2014**, *50*, 10680–10682. [[CrossRef](#)] [[PubMed](#)]
14. Wang, L.-S. Photoelectron Spectroscopy of Size-Selected Boron Clusters: From Planar Structures to Borophenes and Borospherenes. *Int. Rev. Phys. Chem.* **2016**, *35*, 69–142. [[CrossRef](#)]
15. Wang, Y.-J.; You, X.-R.; Chen, Q.; Feng, L.-Y.; Wang, K.; Ou, T.; Zhao, X.-Y.; Zhai, H.-J.; Li, S.-D.; Wu, Y.B.; et al. Chemical Bonding and Dynamic Fluxionality of a B_{15}^+ Cluster: A Nanoscale Double-Axle Tank Tread. *Phys. Chem. Chem. Phys.* **2016**, *18*, 15774–15782. [[CrossRef](#)] [[PubMed](#)]
16. Martínez-Guajardo, G.; Luis Cabellos, J.; Díaz-Celaya, A.; Pan, S.; Islas, R.; Chattaraj, P.K.; Heine, T.; Merino, G. Dynamical Behavior of Borospherene: A Nanobubble. *Sci. Rep.* **2015**, *5*, 11287. [[CrossRef](#)] [[PubMed](#)]
17. Averkiev, B.B.; Zubarev, D.Y.; Wang, L.-M.; Huang, W.; Wang, L.-S.; Boldyrev, A.I. Carbon Avoids Hypercoordination in CB_6^- , CB_6^{2-} , and $C_2B_5^-$ Planar Carbon–Boron Clusters. *J. Am. Chem. Soc.* **2008**, *130*, 9248–9250. [[CrossRef](#)] [[PubMed](#)]
18. Li, W.-L.; Jian, T.; Chen, X.; Chen, T.-T.; Lopez, G.V.; Li, J.; Wang, L.-S. The Planar CoB_{18}^- Cluster as a Motif for Metallo-Borophenes. *Angew. Chem. Int. Ed.* **2016**, *55*, 7358–7363. [[CrossRef](#)] [[PubMed](#)]
19. Liu, L.; Moreno, D.; Osorio, E.; Castro, A.C.; Pan, S.; Chattaraj, P.K.; Heine, T.; Merino, G.; Nguyen, K.A.; Su, S.J.; et al. Structure and Bonding of IrB_{12}^- : Converting a Rigid Boron B_{12} Platelet to a Wankel Motor. *RSC Adv.* **2016**, *6*, 27177–27182. [[CrossRef](#)]
20. Supady, A.; Blum, V.; Baldauf, C. First-Principles Molecular Structure Search with a Genetic Algorithm. *J. Chem. Inf. Model.* **2015**, *55*, 2338–2348. [[CrossRef](#)] [[PubMed](#)]
21. Popov, I.A.; Jian, T.; Lopez, G.V.; Boldyrev, A.I.; Wang, L.-S. Cobalt-Centred Boron Molecular Drums with the Highest Coordination Number in the $CoB_{16}(-)$ Cluster. *Nat. Commun.* **2015**, *6*, 8654. [[CrossRef](#)] [[PubMed](#)]
22. Sergeeva, A.P.; Averkiev, B.B.; Zhai, H.-J.; Boldyrev, A.I.; Wang, L.-S. All-Boron Analogues of Aromatic Hydrocarbons: B_{17}^- and B_{18}^- . *J. Chem. Phys.* **2011**, *134*, 224304. [[CrossRef](#)] [[PubMed](#)]
23. Clark, S.J.; Segall, M.D.; Pickard, C.J.; Hasnip, P.J.; Probert, M.I.J.; Refson, K.; Payne, M.C. First Principles Methods Using CASTEP. *Z. Krist. Cryst. Mater.* **2005**, *220*, 567–570. [[CrossRef](#)]
24. Alexandrova, A.N.; Boldyrev, A.I.; Zhai, H.J.; Wang, L.S. All-Boron Aromatic Clusters as Potential New Inorganic Ligands and Building Blocks in Chemistry. *Coord. Chem. Rev.* **2006**, *250*, 2811–2866. [[CrossRef](#)]
25. Feng, L.-Y.; Zhai, H.-J. Wheel-Like, Elongated, Circular, and Linear Geometries in Boron-Based C_nB_{7-n} ($n = 0-7$) Clusters: Structural Transitions and Aromaticity. *Phys. Chem. Chem. Phys.* **2017**, *19*, 24284–24293. [[CrossRef](#)] [[PubMed](#)]

